Journal of Magnetic Resonance **145,** 302–306 (2000)
doi:10.1006/jmre.2000.2097, available online at http://www.idealibrary.com on IDEAL®

Intermolecular Dipole–Dipole Relaxation of ^{129}Xe Dissolved in Water

Ivan E. Dimitrov, Ravinder Reddy,* and John S. Leigh*

*Department of Biochemistry and Molecular Biophysics and *Department of Radiology, University of Pennsylvania, Philadelphia, Pennsylvania 19104*

Received December 7, 1999; revised March 17, 2000

Intermolecular ^{129}Xe–^{1}H nuclear Overhauser effects and ^{129}Xe longitudinal relaxation time measurements were used to demonstrate that the dipole–dipole coupling is the dominant relaxation mechanism for ^{129}Xe in water, at room temperature. ^{129}Xe–^{1}H cross-relaxation rates were derived to be $\sigma_{XeH} \sim 3.2 \pm 0.3 \times 10^{-3}$ s^{-1}, independent of xenon pressure (in the range of 1–10 bar) and of the presence of oxygen. Corresponding xenon–proton internuclear distances were calculated to be 2.69 ± 0.12 Å. Using the magnitude of the dipole–dipole coupling and the spin density ratio between dissolved xenon and bulk water, it is estimated that ^{129}Xe–^{1}H spin polarization-induced nuclear Overhauser effects would yield little net proton signal enhancement in water.

Key Words: **xenon; water; dipole–dipole coupling; NOE; NMR.**

INTRODUCTION

The low sensitivity of NMR often necessitates utilization of signal enhancement techniques. In most conventional techniques, the enhancement is a result of polarization transfer from a more sensitive spin *S* to an insensitive spin *I*. This scheme is based on the fact that population differences, and thus polarization transfer capacities, are larger for *S* than for *I*, in the same magnetic field. For solution NMR, spin polarization-induced nuclear Overhauser effect (SPINOE) seems to be one exception, with polarization being transferred from the less sensitive but hyperpolarized ^{129}Xe to the more sensitive proton spins. Proton enhancements have been successfully generated in few molecules that either interact directly with or are accessible to xenon (*1–4*), thus pointing to the potential of SPINOE to facilitate high-sensitivity structural and dynamic NMR studies. ^{13}C SPINOE in solutions has also been demonstrated (*3*).

The SPINOE is possible when xenon relaxes through dipole–dipole interactions with the solute (or the solvent) protons. However, a study by Stith *et al.* (*5*) shows that the mere existence of proton-induced enhancement of the xenon relaxation does not necessarily render the SPINOE observable. Other competing mechanisms (relaxation by paramagnetic impurities, spin-rotation, surface interactions, chemical shift anisotropy) can reduce the polarization transferred substantially. Therefore, the *dipolar* contribution to the xenon relaxation must be significant if SPINOE is to be detected.

There is controversy in the literature as to the role the dipole–dipole interaction plays in relaxing ^{129}Xe in solutions. A study of xenon relaxation in deuterated vs protonated isotropic solvents has concluded that intermolecular dipole–dipole interactions are not a dominant relaxation mechanism (*6*); spin-rotation interactions are thought to be the dominant mechanism (*7*). However, the nature of the study in Ref. (*6*) (temperature dependence of T_1^{Xe}) allows one to infer only that spin-rotation may play a role in relaxing xenon in solutions. No quantitative conclusion can be drawn as to what the *dominant* relaxation mechanism is. Moschos and Reisse (*8*) show that the dipole–dipole relaxation is far from negligible, constituting up to 60% of the xenon relaxation in some cases. Computer simulations also support the conjecture that the intermolecular dipole–dipole interactions contribute significantly to the ^{129}Xe relaxation (*9*). Moreover, the successful examples of SPINOE in solutions prove the existence of significant ^{129}Xe–^{1}H dipolar coupling. In addition, a study of xenon dissolved in deuterated solutions of phosphatidylcholine lipid membranes has demonstrated pronounced ^{129}Xe–{^{1}H–lipid} cross-relaxation (*10*). The ^{129}Xe–{^{1}H–water} cross-relaxation, however, was found to be negligibly weak. [The value for the xenon–water cross-relaxation rate derived in that study was most probably underestimated, due to the assumption that the ^{129}Xe spins relax only by dipole–dipole coupling with ^{1}H. Since oxygen was not removed from the samples, it could have served as an efficient polarization sink, thus reducing the value of the *apparent* xenon–proton cross-relaxation.] It is worth noting here that all cited experimental investigations have relied on data derived from using fully or partially deuterated solvents. In such systems, the xenon–solvent dipole–dipole interactions have been heavily suppressed or altogether eliminated, thereby widening the error bars on the values of the xenon–{solvent protons} cross-relaxation. Clearly, additional studies of xenon relaxation in solutions are needed in order to clarify the existing uncertainties in the literature.

In this report, the contribution of the dipolar interaction to the relaxation of ^{129}Xe in water is examined. The choice of water as a system to be investigated seems natural, given that water is the ubiquitous biologically relevant solvent. Protonated, rather than deuterated, water is used as a solvent, in order to facilitate the observation of the ^{129}Xe–^{1}H cross-relaxation. Existence of cross-relaxation between ^{129}Xe and the water

1090-7807/00 $35.00

protons is demonstrated. The contribution of the dipolar coupling on the xenon relaxation is shown to be significant. The cross-relaxation is observed to be pressure independent, in the range of 1–10 bar. Calculations of intermolecular xenon–proton distances are carried out, and the feasibility of xenon–water SPINOE is shortly discussed.

EXPERIMENTAL

Three samples were prepared by pressurizing 2 ml deionized water (v/v 90% H_2O/10% D_2O) with thermally populated natural abundance xenon (26% ^{129}Xe) at pressures of 1, 5, or 10 bar. The 10% D_2O was added in order to lock the spectrometer. Oxygen was removed from the samples by the following procedure: the high-pressure NMR tubes were first pressurized with xenon and the gas was let exchange with the oxygen in the sample for about a minute; the gas was then quickly flushed out and the tube was pressurized with xenon again. This procedure was repeated three times before the tubes were finally sealed. Given the ratio of the volume of the sample to the volume of the NMR tube ($\approx$0.2), the procedure is estimated to yield a 99% reduction of O_2 in the sample. A fourth sample, with 2 bar xenon, was prepared by releasing some of the pressure from the already prepared 5-bar sample, in order for a small amount of O_2 to enter the sample. A fifth sample was prepared with 10 bar xenon and 1 bar O_2. All samples were allowed to equilibrate for at least 2 h before NMR measurements were carried out.

All NMR experiments were conducted at 293 K on a Bruker-AMX500 spectrometer, operating at 138.339 and 500.132 MHz for the ^{129}Xe and ^{1}H resonances, respectively. A 10-mm broadband inverse probe was used, with a nominal ^{129}Xe π/2-pulse of 38 μs. Depending on the sample pressure, one to eight signals were averaged in order to get adequate signal-to-noise ratio.

The intermolecular ^{129}Xe–{^{1}H} NOE was detected using a truncated-driven NOE pulse sequence: TR–$P_\tau(^1\mathrm{H})$–$P_{\pi/2}$ (^{129}Xe)–Acq (^{129}Xe), where $P_\tau(^1\mathrm{H})$ was a pulse train applied for a period τ in order to saturate the water magnetization. $P_{\pi/2}(^{129}\mathrm{Xe})$ was a π/2-pulse applied to ^{129}Xe and followed by the acquisition of the ^{129}Xe free-induction decay. The saturation pulse train consisted of a number of low-power 40-ms long nonselective pulses interleaved with 5-ms delays. The $B_1(^1\mathrm{H}) = 440$ Hz. The saturation period τ was varied by changing the number of these pulse–delay units. The recycle delay, TR, was at least $5 \times T_1^{Xe}$. The NOE curves were obtained by running the saturation time τ with values of up to 700 s, in a randomized order. Off-resonance, control experiments in which the protons were irradiated using 25-kHz off-resonance saturation pulses were also carried out. T_1 measurements were performed using conventional inversion-recovery sequence. Spectra were weighted with an exponential line broadening of 1 Hz. Data analysis was carried out on sets of 10–15 spectra, using a three-parameter nonlinear least squares fit based on the Levenberg–Marquardt algorithm (*11*).

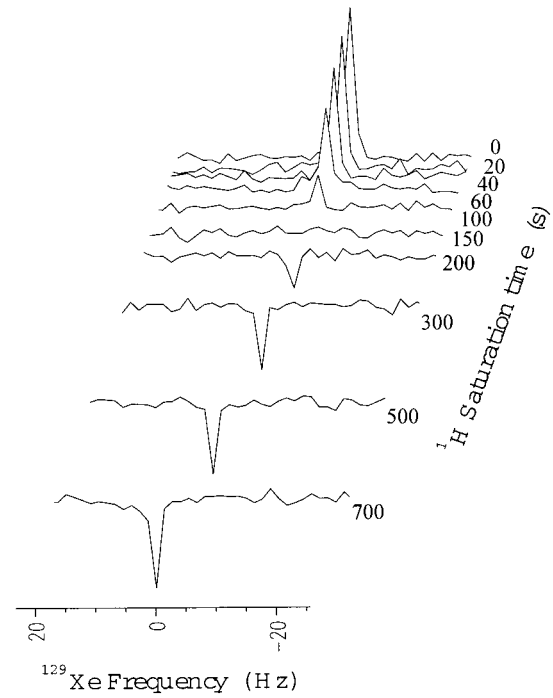

FIG. 1. ^{129}Xe NMR spectra plotted as a function of ^{1}H saturation time. The signal decrease and inversion are results of "negative" intermolecular ^{129}Xe–{^{1}H} NOE.

RESULTS

The truncated-driven NOE pulse sequence allowed for observation of the intermolecular dipole–dipole ^{129}Xe–^{1}H cross-relaxation. Figure 1 shows typical NOE data. The ^{129}Xe signal decreases during the NOE build-up as a result of the negative γ_H/γ_{Xe} ratio and as expected for the case of extreme narrowing. [Molecular dynamics simulations show that the correlation time of xenon in benzene is $\tau_c \sim 5$ ps (*9*). The fluctuations of the xenon–water interactions are expected to be modulated predominantly by translational diffusion, similar to the interaction fluctuations in benzene, with $\omega_H\tau_c \ll 1$.] In fact, the xenon population is partially inverted for long saturation times.

In Fig. 2, $f_{Xe}(\tau) = (I_z(\tau) - I_0)/I_0$ is the fractional signal change after saturation time τ. I_0 and $I_z(\tau)$ are the ^{129}Xe z-magnetizations at equilibrium and after saturation time τ, respectively. All data points were scaled to the magnitude of the xenon spectrum when no proton saturation was applied. As seen, the data follow the expected exponential time dependence. Off-resonance saturation results in no change of the xenon spectrum (open squares in Fig. 2), thus confirming that the observed "negative" NOE is not an artifact.

An estimation of the relative contribution of the dipolar

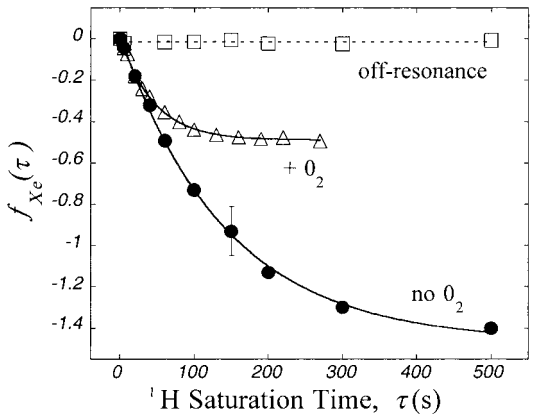

FIG. 2. Fractional change of the xenon magnetization as a function of the proton saturation time. Data shown is for the 10-bar sample. The error bars denote the standard deviation of three measurements. [Only the bars for $f \approx -1$ are seen, since the signal there is within the noise level.] Solid lines are the fits obtained from Eq. [2]. The dashed line serves as a guide to the eye.

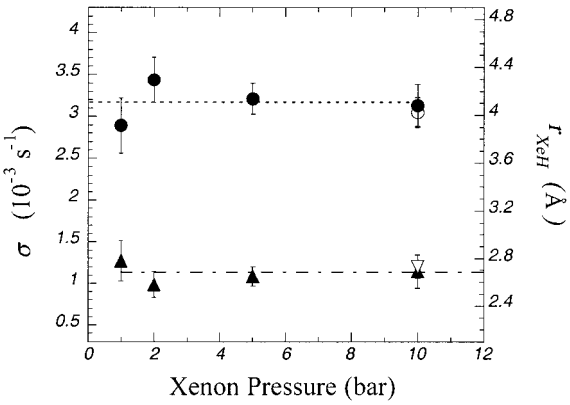

FIG. 3. σ_{XeH} (circles) and $\langle r_{XeH} \rangle$ (triangles) as a function of xenon pressure. The open symbols are for the sample with 1 bar oxygen. The dotted lines are the average values of σ_{XeH} and $\langle r_{XeH} \rangle$.

relaxation to the overall xenon relaxation can be obtained as follows. In the extreme narrowing limit (*12*),

$$f_{eq} = \frac{\gamma_H T_1}{2\gamma_{Xe} T_{dd}} = f_{max} \frac{T_1}{T_{dd}}, \qquad [1]$$

where f_{eq} is the fractional change after long saturation times (equilibrium), and f_{max} ($= -1.79$) is the maximum theoretical change. T_1 and T_{dd} are the total and the dipole–dipole relaxation times, respectively. Estimation of f_{eq} from the fits to the NOE curves, and measurement of T_1 allows for calculation of T_{dd} from Eq. [1]. [The fits to the NOE curves were obtained using Eq. [2]; see below.] Data for all samples are given in Table 1. The ratio of the dipole relaxation rate R_{dd} to the total relaxation rate R_1 shows that, indeed, the ^{129}Xe–^{1}H dipole–dipole relaxation plays a significant (up to 83%) role in relaxing xenon in water. Given the fact that oxygen was not completely removed even from the samples with longest T_1, and that the NMR tubes were not treated as to reduce any surface-induced relaxation, we expect the dipole–dipole interactions to be even more dominant relaxation mechanisms. As seen, T_{dd} is rather independent of the pressure of the gas and of the presence of oxygen, within the experimental errors. T_1^{Xe} is seen to be very sensitive to the presence of O_2, thus confirming previous studies which show that T_1^{Xe} is shortened by interaction with oxygen (*7, 13*). The presence of paramagnetic O_2 also reduces the observed f_{eq} and must therefore be minimized if significant NOE is to be observed.

The ^{129}Xe–^{1}H cross-relaxation rates can be obtained from the recorded NOE data, based on the following solution of the Solomon equations (*14, 15*):

$$f_{Xe}(\tau) = \frac{\gamma_H}{\gamma_{Xe}} \sigma_{XeH} T_1^{Xe} [1 - e^{-\tau/T_1^{Xe}}]. \qquad [2]$$

This solution is valid when the polarization of the protons is constant, as in the case of truncated-driven NOE, where the water is fully saturated during the entire NOE build-up. The second assumption validating Eq. [2] is that the initial ^{129}Xe z-magnetization $I_z(0)$ is equal to its Boltzmann-equilibrium magnitude I_0. Measurement of $f_{Xe}(\tau)$ and T_1^{Xe} allows for calculation of the Xe–H cross-relaxation rate, σ_{XeH}, from Eq. [2]. Data are shown in Table 1 and Fig. 3. The errors in σ_{XeH} (and r_{XeH}, see below) are obtained by measuring the standard deviation in the NOE data points and then performing computerized error propagation analysis. As seen, σ_{XeH} is rather insensitive to the presence of O_2 or to the xenon pressure. Our results indicate that the ^{129}Xe–{^{1}H–water} cross-relaxation

TABLE 1
Dipolar Contribution in Relaxing ^{129}Xe, Cross-Relaxation Rates, and Internuclear Distances for Different Pressures of Xenon

Pressure (bar)	T_1 (s)	f_{eq}	T_{dd} (s)	R_{dd}/R_1 (%)	σ_{XeH} (10^{-3} s^{-1})	r_{XeH} (Å)
1	137 ± 4	−1.43	172 ± 5	80 ± 3	2.9 ± 0.3	2.78 ± 0.17
2	99 ± 4	−1.18	151 ± 6	66 ± 4	3.4 ± 0.3	2.58 ± 0.11
5	131 ± 6	−1.50	157 ± 7	83 ± 5	3.2 ± 0.2	2.65 ± 0.08
10	132 ± 5	−1.46	161 ± 6	82 ± 4	3.1 ± 0.3	2.69 ± 0.14
10 (+O_2)	44 ± 1	−0.49	162 ± 4	27 ± 1	3.0 ± 0.2	2.73 ± 0.10

rates, although modest, are not negligibly weak, somewhat contrary to the observation in the lipid membrane system (*10*). The value of σ_{XeH} for 1 bar is 62% higher than the value estimated by Xu and Tang (*10*).

The ensemble average Xe–H distance, $\langle r_{XeH}\rangle$, can be estimated as follows. The general expression for the cross-correlation rate is

$$\sigma = K^2 I(I+1)\left\{-\frac{1}{12}J_0(\omega_{Xe}-\omega_H)+\frac{3}{4}J_2(\omega_{Xe}+\omega_H)\right\}, \quad [3]$$

where $K = (\mu_0/4\pi)\gamma_H\gamma_{Xe}\hbar$, $I = \frac{1}{2}$, and $J(\omega)$ is the spectral density function (*16*). Both the rotational, σ_{rot}, and the translational, σ_{tr}, contributions to the cross-relaxation are described by Eq. [3], but the expressions for $J(\omega)$ are different for the different contributions. For the rotational relaxation $J_0(\omega) = (24/15)(1/\langle r^6_{XeH}\rangle)(\tau_c/(1+\omega^2\tau_c^2))$ and $J_2(\omega) = (16/15)(1/\langle r^6_{XeH}\rangle)(\tau_c/(1+\omega^2\tau_c^2))$ (*16*). In the extreme narrowing limit, the frequency dependence of the spectral density functions can be ignored leading to $\sigma_{rot} = \frac{1}{2}K^2(\tau_c/\langle r^6_{XeH}\rangle)$. The rotational correlation time, τ_c, can be related to the rotational diffusion constant $\tau_c = 1/(6D_{rot})$ (*15*). D_{rot} is given by Stoke's equation for rotational diffusion $D_{rot} = kT/8\pi\eta r^3_{Xe}$, where k is the Boltzmann constant, T is the temperature, η is the water viscosity, and r_{Xe} is the xenon radius. Therefore, $\tau_c = 4/3(\pi r^3_{Xe})(\eta/kT)$, and

$$\sigma_{rot} = \frac{2}{3}\pi K^2\frac{\eta}{kT}\frac{r^3_{Xe}}{\langle r^6_{XeH}\rangle}. \quad [4]$$

For the translational relaxation, $J_0 = 48/15(\pi J)$ and $J_2 = 32/15(\pi J)$, where $J = (N_H/15D_{tr})(1/\langle r_{XeH}\rangle)$ (*16*). D_{tr} is given by Stoke's equation for the translational diffusion $D_{tr} = kT/6\pi\eta r_{Xe}$. N_H is the number of proton spins that are causing the xenon spins to relax (in spins per m^3). Substituting these expressions for J_0 and J_2 into Eq. [3] one gets

$$\sigma_{tr} = \frac{2}{5}\pi^2 K^2\frac{\eta}{kT}N_H\frac{r_{Xe}}{\langle r_{XeH}\rangle}. \quad [5]$$

Therefore,

$$\sigma_{XeH} = \sigma_{rot}+\sigma_{tr} = \frac{2}{3}\pi K^2\frac{\eta}{kT}\frac{r^3_{Xe}}{\langle r^6_{XeH}\rangle}\left[1+\frac{3}{5}\pi N_H\frac{\langle r^5_{XeH}\rangle}{r^2_{xe}}\right]. \quad [6]$$

Using $\eta_{water} = 1.04\times10^{-3}$ N · s/m^2 (at 293 K) and $r_{Xe} = 2.19$ Å one can estimate $\langle r_{XeH}\rangle$ from Eq. [6]. The results are given in Table 1 and Fig. 3. Given the crudeness of the approximations used in deriving Eq. [6], one should view the values of $\langle r_{XeH}\rangle$ only as a qualitative estimate of the internuclear xenon-proton distances. The values of $\langle r_{XeH}\rangle$ are seen to be invariable over the range of pressures used. The presence of oxygen does not seem to effect $\langle r_{XeH}\rangle$ either. Substituting the obtained values of $\langle r_{XeH}\rangle$ in the expression in the brackets of Eq. [6] reveals that the translational contribution to the cross-relaxation is about 3.5 times that of the rotational contribution. This result is not surprising, since the dissolved xenon is expected to relax predominantly by *inter*molecular interactions.

DISCUSSION

On the basis of our data, we can conclude that the dominant relaxation mechanism for xenon, in protonated water and at room temperature, is dipole–dipole coupling with the solvent protons. These results are in qualitative agreement with a previous study by Moschos and Reisse (*8*). Furthermore, the conclusions we draw do not disagree with the inferences by Diehl and Jokisaari (*6*), since their study was carried out at higher temperatures, where spin-rotation may indeed dominate the relaxation.

Having shown the existence of significant ^{129}Xe–^{1}H dipole–dipole interaction, the feasibility of xenon–water proton SPINOE is now discussed. Solving the Solomon equations for the maximum proton fractional change gives

$$f_{H,max} = -\frac{\gamma_{Xe}}{\gamma_H}\sigma_{HXe}T_1^H f_{Xe}(0). \quad [7]$$

The σ_{HXe} cross-relaxation rate can be calculated as follows. At equilibrium, the total cross-relaxation rates must be equal, $S(S+1)N_H\sigma_{HXe} = I(I+1)N_{Xe}\sigma_{XeH}$, where N denotes the spin density number, and S and I are the proton and xenon spin quantum numbers, respectively. Using 10 bar isotopically enriched xenon (80%) gives $N_{Xe}/N_H = 3\times10^{-4}$, and $\sigma_{HXe} = \sigma_{XeH}N_{Xe}/N_H \sim 10^{-6}$ s^{-1}. [$N_{Xe} = 43$ mM, since xenon concentration is expected to be directly proportional to pressure, in accordance with Henry's law (*17*).] Substituting $\sigma_{HXe} \sim 10^{-6}$ s^{-1} and $f_{Xe}(0) \sim 2\times10^4$ (10% hyperpolarization) in Eq. [7], one obtains $f_{H,max} \sim 10^{-2}$. [$T_1^H \sim 2.2$ s was obtained for the 5-bar sample; similar or shorter T_1^H are expected for the rest of the samples.] This is a small enhancement indeed. We therefore conclude that, although the cross-relaxation exists, its magnitude is such that, at the given concentration of xenon in *bulk* water, very little net water proton signal enhancement would be expected.

A way to circumvent the limitation presented by the shear number of protons in bulk water would be to raise the interfacial water–xenon contacts. Perhaps, this could be done using hydrophilic hollow-fiber artificial capillary systems (*18, 19*). These bioreactors consist of a large number of porous capillaries, thus creating large surface areas (2000 cm^2/cartridge). Based on these characteristics, an enhanced hyperpolarization transfer scheme can be envisioned, where the *number* of the

coupled ^{129}Xe–{^{1}H–water} spins would be increased. It appears therefore, that xenon's dipole–dipole coupling with ^{1}H and its implications for studying water-soluble molecules using transfer of hyperpolarization merit further considerations.

ACKNOWLEDGMENTS

We thank L. Mayne and S. W. Englander for providing us with spectrometer time and for their help with the NOE experiments. This work was supported by NIH Grant RR02305.

REFERENCES

1. G. Navon, Y.-Q. Song, T. Rõõm, S. Appelt, R. E. Taylor, and A. Pines, Enhancement of solution NMR and MRI with laser-polarized xenon, *Science* **271,** 1848–1851 (1996).
2. Y.-Q. Song, B. M. Goodson, R. E. Taylor, D. D. Laws, G. Navon, and A. Pines, Selective enhancement of NMR signals for α-cyclodextrin with laser-polarized xenon, *Angew. Chem. Int. Ed. Engl.* **36,** 2368–2370 (1997).
3. R. J. Fitzgerald, K. L. Sauer, and W. Happer, Cross-relaxation in laser-polarized liquid xenon, *Chem. Phys. Lett.* **284,** 87–92 (1998).
4. M. Luhmer, B. M. Goodson, Y.-Q. Song, D. D. Laws, L. Kaiser, M. C. Cyrier, and A. Pines, Study of xenon binding in cryptophane-A using laser-induced NMR polarization enhancement, *J. Am. Chem. Soc.* **121,** 3502–3512 (1999).
5. A. Stith, T. K. Hitchens, D. P. Hinton, S. S. Berr, B. Driehuys, J. R. Brookeman, and R. G. Bryant, Consequences of ^{129}Xe–^{1}H cross relaxation in aqueous solutions, *J. Magn. Reson.* **139,** 225–231 (1999).
6. P. Diehl and J. Jokisaari, Nuclear magnetic relaxation of the ^{129}Xe and ^{131}Xe isotopes of xenon gas dissolved in isotropic and anisotropic liquids, *J. Magn. Reson.* **88,** 660–665 (1990).
7. H. C. Torrey, Chemical shift and relaxation of Xe^{129} in xenon gas, *Phys. Rev.* **130,** 2306–2312 (1963).
8. A. Moschos and J. Reisse, Nuclear magnetic relaxation of xenon-129 dissolved in organic solvents, *J. Magn. Reson.* **95,** 603–606 (1991).
9. M. Luhmer, A. Moschos, and J. Reisse, Intermolecular dipole–dipole spin relaxation of xenon-129 dissolved in benzene. A molecular-dynamics simulation study, *J. Magn. Reson. A* **113,** 164–168 (1995).
10. Y. Xu and P. Tang, Amphiphilic sites for general anesthetic action? Evidence from ^{129}Xe–{^{1}H} intermolecular nuclear Overhauser effects, *Biochim. Biophys. Acta* **1323,** 154–162 (1997).
11. P. R. Bevington, "Data Reduction and Error Analysis for the Physical Sciences," McGraw–Hill, New York (1969).
12. T. C. Farrar and E. D. Becker, "Pulse and Fourier Transform NMR," Academic Press, New York (1973).
13. C. J. Jameson, A. K. Jameson, and J. K. Hwang, Nuclear spin relaxation by intermolecular magnetic dipole coupling in the gas phase. ^{129}Xe in oxygen, *J. Chem. Phys.* **89,** 4074–4081 (1988).
14. I. Solomon, Relaxation processes in a system of two spins, *Phys. Rev.* **99,** 559–565 (1955).
15. J. H. Noggle and R. E. Schirmer, "The Nuclear Overhauser Effect: Chemical Applications," Academic Press, New York (1971).
16. A. Abragam, "The Principles of Nuclear Magnetism," Oxford Univ. Press, London (1961).
17. "IUPAC Solubility Data Series," Vol. 2 (H. L. Clever, Ed.), Pergamon Press, Oxford (1979).
18. O. Kaplan, P. C. M. van Zijl, and J. S. Cohen, NMR studies of metabolism of cells and perfused organs, *in* "NMR: Basic Principles and Progress" (J. Seelig and M. Rudin, Eds.), Vol. 28, pp. 3–52, Springer-Verlag, Berlin (1992).
19. K. A. McGovern, Bioreactors, *in* "NMR in Physiology and Biomedicine" (R. J. Gillies, Ed.), pp. 279–293, Academic Press, San Diego (1994).